



# HHS Public Access

## Author manuscript

AAPS PharmSciTech. Author manuscript; available in PMC 2019 August 01.

Author Manuscript

Author Manuscript

Author Manuscript

Author Manuscript

Published in final edited form as:

*AAPS PharmSciTech*. 2018 August ; 19(6): 2700–2709. doi:10.1208/s12249-018-1095-z.

## Chronotherapeutic Drug Delivery of Ketoprofen and Ibuprofen for Improved Treatment of Early Morning Stiffness in Arthritis Using Hot-Melt Extrusion Technology

Nagi Reddy Dampa<sup>1</sup>, Sandeep Sarabu<sup>1</sup>, Suresh Bandari<sup>1</sup>, Feng Zhang<sup>2</sup>, and Michael A. Repka<sup>1,3,4</sup>

<sup>1</sup>Department of Pharmaceutics and Drug Delivery, School of Pharmacy, The University of Mississippi, University, Oxford, Mississippi 38677, USA

<sup>2</sup>College of Pharmacy, The University of Texas at Austin, Austin, Texas 78712, USA

<sup>3</sup>Pii Center for Pharmaceutical Technology, The University of Mississippi, University, Oxford, Mississippi 38677, USA

### Abstract

This work developed a chronotherapeutic drug delivery system (CTDDS) utilizing a potential continuous hot-melt extrusion (HME) technique. Ketoprofen (KTP) and ibuprofen (IBU) were used as two separate model drugs. Eudragit S100 (ES100) was the matrix-forming agent, and ethyl cellulose (EC) (2.5 and 5%) was the release-retarding agent. A 16-mm extruder was used to develop the CTDDS to pilot scale. The obtained extrudate strands were transparent, indicating that the drugs were homogeneously dispersed in the matrix in an amorphous form, confirmed by both differential scanning calorimetry and powder X-ray diffraction. The strands were pelletized into 1, 2, and 3 mm size pellets. A 100% drug release from 1, 2, and 3 mm pellets with 2.5% EC was observed at 12, 14, and 16 h, whereas the drug release was sustained for 14, 16, and 22 h from 5% EC pellets, respectively, for KTP. The release characteristics of IBU were similar to those of KTP with modest variations in release at lag time. The *in vitro* drug release study conducted in three-stage dissolution media showed a desired lag time of 6 h. The percent drug release from 1, 2, and 3 mm pellets with 40% drug load showed < 20% release from all formulations at 6 h. The amount of ethyl cellulose and pellet size significantly affected drug release. Formulations of both KTP and IBU were stable for 4 months at accelerated stability conditions of 40°C/75% RH. In summary, HME is a novel technique for developing CTDDS.

### Keywords

chronotherapeutic; drug delivery; arthritis; hot-melt extrusion; Eudragit S 100

<sup>4</sup>To whom correspondence should be addressed. (marepka@olemiss.edu).

## INTRODUCTION

Chronotherapeutics deals with synchronizing drug delivery with the body's circadian rhythm to optimize therapeutic efficacy and minimize side effects (1). Diseases that follow the circadian rhythm with exacerbated symptoms at specific times of the day are targets of chronotherapeutic drug delivery systems (CTDDS). Various diseases that follow the circadian rhythm include rheumatoid arthritis, cardiovascular disorders, bronchial asthma, gastric ulcers, cancer, and some neurological disorders (2). Among the diseases that follow circadian rhythms, arthritis is a condition characterized by exacerbated pain, joint stiffness, and swelling of the fingers in the early morning hours due to the presence of high concentrations of c-reactive protein and interleukin-6 in the plasma (3). Thus, the chronotherapeutic delivery of nonsteroidal anti-inflammatory drugs (NSAIDs) such as ketoprofen (KTP) and ibuprofen (IBU) could improve the quality of life of arthritis patients.

Recently, there has been a growing interest in chronotherapeutic drug delivery systems (CTDDS) with the advantage of delivering drugs at a specific time to a specific site (4). These CTDDS avoid first pass metabolism, minimize drug side effects, and mainly deliver drugs following the body's circadian rhythm after a pre-determined lag time when the peak plasma concentration of the drug is required. Several researchers have formulated chronotherapeutic and pulsatile drug delivery systems using different strategies. Nayak *et al.* developed a pulsatile capsule dosage form of valsartan as a treatment model for the early morning surge in blood pressure (5). Jose *et al.* formulated colon-specific chitosan microspheres for chronotherapy of chronic stable angina (6). Shiohira *et al.* prepared a chronotherapeutic rectal aminophylline delivery system for asthma therapy (7). Recently, Haiying *et al.* developed a time-adjustable pulsatile system (TAPS) for the treatment of arthritis (8). Although many strategies have been developed for formulating chronotherapeutic and pulsatile drug delivery systems, most of them are not suitable for scale up or for a continuous manufacturing process because their production requires several complex steps and the inclusion of solvents, is time consuming, and demands increased manufacturing costs. Therefore, we aimed to develop a CTDDS of KTP and IBU using the continuous hot-melt extrusion (HME) technique.

HME technology has gained significant attention in pharmaceutical research and manufacturing in the last two decades owing to its inherent advantages of process automation, fewer processing steps, being solvent free, and reduced required capital investment (9,10). HME offers additional advantages including taste masking, abuse deterrence, shaped delivery systems, 3D-printing, solubility, and bioavailability enhancement (11). HME is widely used in solubility enhancement and formulation of various dosage forms, including immediate release tablets (12–14), sustained release forms (15,16), transdermal and topical delivery systems (17,18), transmucosal delivery (19,20), solid lipid nanoparticles (21), nanocrystals (22), and colon drug delivery systems (23,24).

KTP and IBU are widely prescribed NSAIDs for the treatment of rheumatoid arthritis. Although these NSAIDs are very effective in relieving pain associated with rheumatoid arthritis, the main disadvantages are the side effects, which include gastric bleeding, dyspepsia, and peptic ulceration (25). Another problem that needs to be addressed regarding

these drugs is their short half-life (26). Owing to the short half-life, the drugs need to be administered just before the onset of symptoms (*i.e.*, in the early morning hours), which leads to patient incompliance. The chronomodulated systems offer an advantage of temporal and site-specific drug release. The reported compression coated and coating drug core chronotherapeutic systems have complex manufacturing processes, which include multiple steps. However, hot-melt extrusion technology was reported as a continuous process with reduced downstream processing (22). Thus, this technology was utilized to produce simple chronomodulated pellets in capsules as an alternative dosage form. To the best of our knowledge, there are no reports of chronotherapeutic drug delivery systems using HME technology for improved chronotherapy for arthritis. A drug delivery system that delivers the drug after a pre-determined lag time (approximately 6 h) and maintains the constant blood plasma concentration is required for better patient compliance and optimal therapeutic efficacy. This requirement can be fulfilled by developing a chronotherapeutic drug delivery system that delivers the drug according to the body's circadian rhythm (27). To achieve this, Eudragit S100 (ES100) was selected as an enteric polymer that solubilizes and releases the drug at above pH 7. Ethyl cellulose (EC) was utilized to provide the desired lag time with slow release and maintain constant blood plasma concentrations thereafter. The main objective of the current investigation was to develop a chronotherapeutic drug delivery system for the NSAIDs KTP and IBU with a desired lag time of 6 h using an industrially feasible continuous HME process.

## MATERIALS AND METHODS

### Materials

KTP and IBU were purchased from PCCA (Houston, Texas). Eudragit S100 (ES100) was a kind gift from Evonik (Darmstadt, Germany), and ethyl cellulose (EC) was obtained from the DOW chemical company (Midland, Michigan). All other reagents used were purchased from Fisher Scientific and were of analytical grade.

### Methods

**HME Processing**—The polymers and drugs were sifted using a sieve (USP #30 screen size) and dried in an oven at 40°C to remove any residual moisture present. The materials were blended using a twin shell V-blender (GlobePharma, Maxiblend®) at 25 rpm for 15 min. Preliminary experiments were performed initially using a 6-mm counter-rotating mini extruder (Haake Minilab, Thermo Electron, Germany), and thereafter optimized formulations were finally extruded using the pilot scale 16-mm co-rotating twin screw extruder with a standard screw configuration as shown in Fig. 1 (16 mm, Prism Euro Lab, Thermo Fisher Scientific). The composition of different formulations, processing parameters, and percent drug released after lag time (6 h) using the 6-mm extruder is listed in Table I. Formulation compositions and processing parameters of experiments on the 16-mm extruder are listed in Table II. Initial extrudates obtained during the extrusion process were discarded until the extruder had attained a steady state, and then extrudates collected were cooled at ambient temperature and pelletized simultaneously using a pelletizer into pellets of 1, 2, and 3 mm in size. The extrudates were also milled using a comminuting mill

(Fitzpatrick, model L1A) and sieved using a USP mesh screen (#25). The pellets were stored in poly bags in a desiccator until further evaluation.

### HPLC Analysis of NSAIDs

**Ketoprofen**—The content of KTP present in the *in vitro* samples was quantified using a HPLC system (Waters Corp, Milford, MA, USA). For KTP (method stated in USP-NF was used), a Phenomenex Luna® C18 reverse phase column (5 µm, 100 Å, 250 × 4.6 mm) was used as the stationary phase. The mobile phase consisted of water, acetonitrile, and glacial acetic acid (90:110:1). The flow rate was maintained at 1.2 mL/min, and the UV-detector was set at 256 nm (Waters 2489 UV/detector). Twenty microliters was injected from each sample, and the data was analyzed using Empower 2 software. A six-point calibration curve was plotted and found to be linear in the concentration range of 2 µg/mL to 100 µg/mL with a correlation coefficient ( $R^2$ ) of 0.999. The limit of detection and limit of quantification values for the method were found to be 0.2 and 0.7 µg/mL, respectively.

**Ibuprofen**—The IBU content was analyzed using a Phenomenex Luna® C18 reverse phase column (5 µm, 100 Å, 250 × 4.6 mm) stationary phase, and the mobile phase consisted of water, acetonitrile, and chloro acetic acid (40:60:0.01) (USP-NF). The flow rate was 2 mL/min, sample volume was 10 µL, and the UV-detector was set at 221 nm (Waters 2489 UV/detector). Empower 2 software was used to analyze the data. A calibration curve plotted was found to be linear in the concentration range of 1 to 100 µg/mL with a correlation coefficient ( $R^2$ ) of 0.999. The limit of detection and limit of quantification values for the method were found to be 0.3 and 1 µg/mL, respectively.

### Solid-State Characterization

**Thermogravimetric Analysis**—The thermal stability of all materials used in formulations was determined using a PerkinElmer Pyris 1 thermogravimetric analyzer (TGA) equipped with Pyris manager software (PerkinElmer Life and Analytical Sciences, 719 Bridgeport Ave., CT, USA). Each sample weighing 3–5 mg was taken and heated at a heating rate of 10°C/min from 20 to 250°C.

**DSC**—A differential scanning calorimeter (DSC 25 Series, TA instruments) was used to assess the thermal characteristics and compatibility of polymers with KTP and IBU. Samples (pure KTP, pure IBU, ES100, EC, physical mixtures, and extrudates) weighing 5–10 mg were hermetically sealed in an aluminum pan and heated at a rate of 10°C/min from 25 to 150°C. Ultra-pure nitrogen was used as the purge gas at a flow rate of 50 mL/min.

**PXRD**—The solid state of KTP, IBU, ES100, EC extrudates, and the respective physical mixtures was investigated using a powder X-ray diffraction apparatus (Bruker AXS, Madison, MI) using CuK $\alpha$  radiation at a 40-kV generator voltage and 40 mA current. The diffraction angles were 5–40° (2 $\theta$ ), and the scanning rate was set at 2°/min.

**FTIR Spectroscopy**—The molecular interactions of KTP and IBU with polymers, before and after HME processing, were analyzed by FTIR spectroscopy. The studies were performed on an Agilent Technologies Cary 660 (Santa Clara, CA) instrument. The bench

Author Manuscript  
Author Manuscript  
Author Manuscript  
Author Manuscript

was equipped with an ATR (Pike Technologies MIRacle ATR, Madison, WI) that was fitted with a single bounce diamond-coated ZnSe internal reflection element. The scanning range was 400–4000 cm<sup>-1</sup>.

**Drug Content**—The extrudates of both KTP and IBU were ground separately into fine powder using a mortar and pestle. An accurately weighed amount equivalent to 50 mg of API (active pharmaceutical ingredient) was transferred into a 50-mL volumetric flask, 50 mL of methanol was added and placed in a sonicator for 30 min (Branson 2510, Branson Ultrasonic Corp., Danbury, CT, USA), and the solution obtained was centrifuged for 15 min at 10000 rpm. Supernatant was collected and diluted with phosphate buffer of pH 7.4 and analyzed for KTP and IBU content separately using HPLC analysis.

**In vitro Dissolution Study**—Three-stage dissolution testing was performed according to the USP XXIII paddle method using an SR8-plus Hanson dissolution apparatus (6,23). Firstly, dissolution was conducted in 750 mL of 0.1 N HCl for 2 h. In the second stage, after 2 h, the pH was increased to 6.8 by addition of 250 mL of 0.2 M sodium triphosphate buffer, and dissolution was carried out for 4 h. In the third stage, the pH of the dissolution medium was adjusted to pH 7.4 with 0.1 M sodium hydroxide, and dissolution was conducted up to 24 h. Paddle rotation was set at 50 rpm, and the temperature of the dissolution medium was maintained at 37 ± 0.5°C. Samples (3 mL) were collected at pre-determined intervals, and KTP and IBU contents were quantified using a HPLC system.

**SEM**—The surface morphology of pellets before dissolution and during dissolution of both KTP and IBU was assessed using a JSM-5600 scanning electron microscope (JEOL USA, Inc., Waterford, VA, US). The pellets at 0 h and at different time points in the dissolution media (2 h in 0.1 N HCl; 6 h in pH 6.8 phosphate buffer; and 7, 10, and 12 h in pH 7.4 phosphate buffer) were collected, placed in a sieve, and air dried for 24 h to remove any water content present. These dried pellets were sputter coated with gold under an argon atmosphere using a Hummer 6.2 Sputter Coater (Ladd Research Industries, Williston, VT, USA), and surface morphology was observed using a JSM-5600 scanning electron microscope at an accelerating voltage of 5 kV.

**Statistical Analysis**—The differences between *in vitro* dissolution results of all formulations extruded using 16 mm were analyzed by one-way analysis of variance (ANOVA). A *p* value 0.05 indicated statistical significance. All values are reported as the mean of three recordings.

**Stability Studies**—Formulations (KTP1-3MM, IBU1-3MM) were stored at accelerated stability conditions (*i.e.*, at 40°C/75% RH). The formulations were evaluated physically and tested for drug content and *in vitro* dissolution release profiles. Physical appearance was observed and noted. The similarity factor was calculated using the following equation:

$$f_2 = 50 \cdot \log \left\{ \left[ 1 + \frac{1}{n} \sum_{t=1}^n (R_t - T_t)^2 \right]^{0.5} \times 100 \right\}$$

$R_t$  and  $T_t$  are the cumulative percentage dissolved at each of the selected  $n$  time points of the reference and test product, respectively. The value of the similarity factor ranges from 1 to 100, and if the values approach 100, the similarity between the test and reference product increases. The similarity factor should be above 50 to consider the test and reference products similar.

## RESULTS AND DISCUSSION

### HME Processing

Preliminary experiments performed using a 6-mm extruder (Haake Minilab, Thermo Electron, Germany) to assess the feasibility of the processing parameters (temperature, feed rate, rpm) provided the data to optimize the conditions without any thermal degradation of the materials used. ES100, KTP, and IBU were selected as the enteric polymer and drugs, respectively. KTP and IBU are frequently indicated in treatment of arthritis (a condition target of the chronotherapeutic drug delivery system). ES100 has a high glass transition ( $T_g$ ) temperature of 172°C, as reported previously (28). KTP and IBU exhibited melting points at 94 and 78°C, respectively (Determined by DSC, TA 25 SERIES). Both KTP and ES100 undergo thermal degradation above 180°C and IBU above 150°C (29). Usually, extrusion of polymers is carried out above the glass transition temperature for the polymer to have sufficient mobility inside the extruder and to maintain the torque value below the maximum level where the motor cannot function. Plasticizers, which increase molecular chain mobility and reduce frictional forces between polymer chains, are used to reduce the glass transition temperature, facilitating smooth HME processing at low temperatures (30). The two model drugs employed in this study, KTP and IBU, can act as plasticizers, so no plasticizers were used in the present study.

In preliminary experiments carried out on a 6-mm extruder, ES100 and KTP were extruded at 30, 40, and 50% drug load. Extrudate strands of 30 and 40% drug load formed a coalesced matrix and were transparent, whereas with 50% drug loading, extrudates were not transparent and the formulation flowed out as a liquid because of the high KTP content. When the processing temperature was further decreased to obtain coalesced extrudate strands, ES100 was observed as distinct particles and phase separation occurred, which can be due to nonmelting of ES100. *In vitro* dissolution testing was carried out for 30 and 40% drug loading of KTP to understand the release pattern (results not shown), and the results showed above 50% within 6 h with no desired lag time, which was not suitable for the desired chronotherapeutic drug delivery system. Similarly, IBU extrudates with ES100 released the maximum drug within 6 h.

In the next stage, EC, a hydrophobic polymer, was added to the formulation (2.5, 5, and 10%) to retard the initial drug release beyond 6 h. The dissolution profile revealed that EC was able to retard the drug with a minimum amount of drug released in the first 6 h (less than 20%). Based on these preliminary experiments and the results for both KTP and IBU, further trials were carried out on a 16-mm extruder with optimized formulations, as one of the objectives of the current investigation was to develop an industrially feasible chronotherapeutic drug delivery system.

KTP with 40% drug loaded with EC (2.5 and 5%) and ES 100 was extruded at a temperature of 120°C, screw speed of 100 rpm, and feed rate of 5 g/min. The extrudates obtained were coalesced and transparent, as shown (Fig. 2a). Similarly, the extrusion was carried out with IBU at 40% drug loading with EC (2.5 and 5%) and ES100 at 100°C, 100 rpm screw speed, and 5 g/min feed rate. The images of the extrudates are shown in Fig. 2b.

### Solid-State Characterization

The TGA results showed that APIs and polymers were stable at the processing temperatures employed during HME. The DSC thermograms of KTP, IBU, ES100, EC, physical mixtures of drug and polymers, and extrudates are shown in Fig. 3. The DSC thermograms of pure KTP and IBU showed sharp endotherms at 78 and 94°C, corresponding to their melting points. The intensities of these peaks were reduced in the physical mixtures (PM). In both the KTP and IBU extrudates, these characteristic endotherms disappeared, indicating the amorphous nature of APIs in the extrudates and the complete miscibility of drugs and polymers. This was further confirmed by the powder X-ray diffraction (PXRD) studies. In PXRD (Fig. 4), KTP had major characteristic peaks at 6.3°, 13.1°, 17.3°, and 22.9°, and IBU showed peaks at 6°, 16.5°, 19.5°, and 22°. The intensities of the peaks were reduced in physical mixtures, and complete absence of peaks was observed in extrudates, in correlation with DSC thermograms, substantiating the amorphous nature of KTP and IBU in the formulations. This conversion of crystalline drugs into an amorphous nature may be attributed to the molecular mixing of components in the molten form during melt extrusion.

### FTIR Spectroscopy

FTIR spectra of pure KTP, IBU, ES100, EC, physical mixtures, and formulations are shown in Fig. 5. FTIR spectra showed major characteristic peaks of KTP at wave numbers 1693, 1653, 1282, 714, and 702 cm<sup>-1</sup>. These major characteristic peaks were observed in the physical mixture and extrudate formulations, suggesting the absence of intermolecular interactions between the drug and other polymers utilized in the formulations. Similarly, IBU had characteristic peaks at 2952, 1709, and 779 cm<sup>-1</sup> both in the physical mixture and formulation compared with pure IBU, indicating absence of interactions. These results suggest the suitability of the materials in the formulation of chronomodulated systems of KTP and IBU for treating early morning symptoms of rheumatoid arthritis.

### In vitro Dissolution Study

The *in vitro* drug release studies performed in different pH conditions to assess the suitable chronotherapeutic formulation showed the desired lag time. In this investigation, formulations with < 20% drug release in 6 h (lag time) were considered to meet the requirements of the optimized chronotherapeutic drug delivery system to relieve the symptoms of rheumatoid arthritis conditions in the early morning. The *in vitro* dissolution profiles of KTP and IBU formulations are shown in Figs. 6 and 7, respectively. The dissolution rate of both the drugs was influenced by the concentration of EC and the size of the extrudate pellets.

### Effect of Pellet Size

The dissolution profile of the drug from different formulations is dependent on the pellet size of the extrudates. In pH 1.2 media after 2 h, less than 0.5% of the drug was released from the KTP pellets compared to approximately 3.4–4.2% drug release observed in the pulverized formulations (KTP1—#25SIEVE and KTP2—#25SIEVE). At the end of 6 h in pH 6.8 buffer, the drug release from different sized pellets with 2.5% EC was in the range of 10.6–15.0%. Similar results were observed with the formulation composed of 5% EC (10.1–14.6%). The formulations, with 2.5% or 5% EC in pH 7.4 media, showed a complete drug release and a sustained drug release from the 3 mm size pellets compared to that from the smaller sized pellets (1 and 2 mm). These results ascertain that the drug release is influenced by the pellet size, as discussed in the earlier literature reports (31,32). Moreover, a complete drug release (90 and 94%) from powdered formulations was observed at pH 6.8, and this was significantly different ( $p < 0.05$ ) than that observed in the pellets. This is attributed to the increased surface area due to the smaller particle size of the powdered formulation. Sustained drug release from the larger pellet size could be attributed to either the lower surface area of the larger pellets compared to the smaller pellets or increased average distance for diffusion of the active ingredient from the pellet (33).

### Effect of Ethyl Cellulose

In addition to pellet size, a remarkable impact of EC composition on drug release behavior was observed. As the composition of the EC increased, the pellets showed more sustained drug release profiles. A 100% drug release from 1, 2, and 3 mm pellets with 2.5% EC was noticed at 12, 14, and 16 h, respectively, while the drug release was sustained for 14, 16, and 22 h, respectively, from pellets containing 5% EC. This marked difference in dissolution profiles of pellets with 2.5 and 5% EC supports the fact that EC maintains the matrix integrity for a longer time at a high concentration. Further, 90 and 94% drug release from the powdered formulations in 6 h could be correlated with the weak matrix integrity due to loss of EC during the pulverization.

Figure 4 delineates the drug release profile of IBU. The dissolution profile data shows that results were in correlation with KTP, with a slight variation in the amount of drug released at lag time. Since 18% drug release was observed from 3 mm pellets (2.5% EC) at lag time (6 h), no other sized pellets of IBU were fabricated and evaluated (as formulations with < 15% drug release at lag time were set to be suitable for chronotherapeutic systems). As observed with the KTP *in vitro* results, the 3 mm pellets of IBU with 2.5% EC showed a 12-h drug release profile while the pellets with 5% EC sustained drug release for 24 h.

From the above *in vitro* dissolution results for KTP and IBU, formulations of KTP1-1MM and IBU1-1MM showed 100% drug release in 12 h, which could relieve the early morning symptoms of arthritis with the required therapeutic concentrations. The 3 mm KTP and 3 mm IBU pellets showed sustained release. The correlation coefficient values of all the formulations of KTP or IBU showed a good correlation to the zero-order equation ( $r^2 = 0.9712$ – $0.9998$ ) and high linearity when compared to other models, suggesting that drug release followed the zero order. From the above results, it can be inferred that a

chronotherapeutic drug delivery system can be developed using HME technology with desired drug release characteristics.

### SEM

SEM images of KTP pellets (Fig. 8i) obtained from the dissolution vessel, at different time points, elucidated the surface morphological changes that occurred during the dissolution process, further confirming the drug release mechanism from the matrix. The intact surface of the 3 mm KTP pellet at pH 1.2 at 2 h (Fig. 8i (b)) ensured low or no drug release. The appearance of small cracks on the surface of the pellets obtained from pH 6.8 media supported the minimum drug release at 6 h (Fig. 8i (c)). The intensity of cracks and the dissolution rate increased as the pH of the dissolution changed to 7.4 (Fig. 8i (d)). The increased intensity of the cracks may be caused by the dissolving nature of the Eudragit at above pH 7. The reduction in pellet size was observed from images taken at 10 and 12 h (Fig. 8i (e, f)). In SEM images of IBU (Fig. 8ii), the film formation by EC on the surface of the pellets was not clearly observed, and the intensity of cracks was less when compared to KTP. A hole formation was observed (Fig. 8ii (f)) in pellets along with a size reduction. This may be caused by a variation in solubility of IBU in the dissolution media compared to KTP.

### Stability Study

The stability of the formulations at accelerated stability conditions (45°C and 75% RH) for both KTP and IBU showed stability over 4 months. The stability samples were characterized for drug release properties and drug content. The *in vitro* drug release studies performed after the 4th month showed similar release profiles compared to those of the initial samples. The similarity factor ( $F_2$ ) value was above 70, confirming the similar release profile and stability. Drug content ( $n = 3$ ) was found to be in the range of 96–103%. Further, the extrudates did not show any change in physical appearance after 3 months of accelerated stability study. Dissolution profiles of formulations KTP1-3MM and IBU1-3MM initially and at 4 months are shown in Fig. 9.

## CONCLUSION

A chronotherapeutic drug delivery system for KTP and IBU was successfully developed for the treatment of arthritis conditions in the early morning hours. The drug release studies conducted in different media showed the desired lag time and release characteristics. The concentration of ethyl cellulose and size of extrudate pellets had significant effects on *in vitro* drug release profiles. Ethyl cellulose at low concentrations of 2.5 and 5% can act as a potent release retarding agent in the HME techniques. Furthermore, the developed formulations need to be assessed *in vivo*. In conclusion, HME is a novel, viable technique suitable for developing a chronotherapeutic drug delivery system with many advantages compared to those of other traditional techniques.

### Acknowledgments

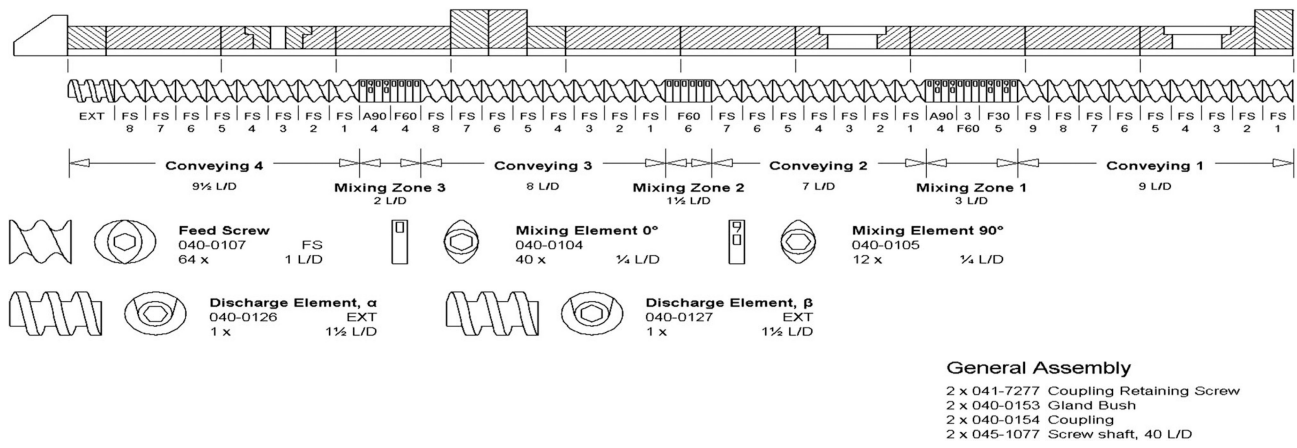
The authors also thank the Pii Center for Pharmaceutical Technology for contributions in this project.

**Funding information** This study was partially supported by Grant Number P20GM104932 from the National Institute of General Medical Sciences (NIGMS), a component of the National Institute of Health (NIH).

## References

1. Khan Z, Pillay V, Choonara YE, Du Toit LC. Drug delivery technologies for chronotherapeutic applications. *Pharm Dev Technol*. 2009; 14(6):602–12. [PubMed: 19883249]
2. Mandal AS, Biswas N, Karim KM, Guha A, Chatterjee S, Behera M, et al. Drug delivery system based on chronobiology—a review. *J Control Release*. 2010; 147(3):314–25. [PubMed: 20691738]
3. Saitoh T, Watanabe Y, Kubo Y, et al. Intragastric acidity and circadian rhythm. *Biomed Pharmacother*. 2001; 55:138–41.
4. Roy P, Shahiwala A. Statistical optimization of ranitidine HCl floating pulsatile delivery system for chronotherapy of nocturnal acid breakthrough. *Eur J Pharm Sci*. 2009; 37(3–4):363–9. [PubMed: 19491027]
5. Nayak UY, Shavi GV, Nayak Y, Averinen RK, Mutualik S, Reddy SM, et al. Chronotherapeutic drug delivery for early morning surge in blood pressure: a programmable delivery system. *J Control Release*. 2009; 136(2):125–31. [PubMed: 19239918]
6. Jose S, Prema MT, Chacko AJ, Thomas AC, Souto EB. Colon specific chitosan microspheres for chronotherapy of chronic stable angina. *Colloids Surf B Biointerfaces*. 2011; 83(2):277–83. [PubMed: 21194900]
7. Shiohira H, Fujii M, Koizumi N, Kondoh M, Watanabe Y. Novel chronotherapeutic rectal aminophylline delivery system for therapy of asthma. *Int J Pharm*. 2009; 379(1):119–24. [PubMed: 19555748]
8. Wang H, Cheng L, Wen H, Li C, Li Y, Zhang X, et al. A time-adjustable pulsatile release system for ketoprofen: in vitro and in vivo investigation in a pharmacokinetic study and an IVIVC evaluation. *Eur J Pharm Biopharm*. 2017; 119:192–200. [PubMed: 28633956]
9. Patil H, Tiwari RV, Repka MA. Hot-melt extrusion: from theory to application in pharmaceutical formulation. *AAPS PharmSciTech*. 2016; 17(1):20–42. [PubMed: 26159653]
10. Repka MA, Bandari S, Kallakunta VR, Vo AQ, McFall H, Pimparade MB, et al. Melt extrusion with poorly soluble drugs—an integrated review. *Int J Pharm*. 2018; 535(1–2):68–85. [PubMed: 29102700]
11. Tiwari RV, Patil H, Repka MA. Contribution of hot-melt extrusion technology to advance drug delivery in the 21st century. *Expert Opin Drug Deliv*. 2016; 13(3):451–64. [PubMed: 26886062]
12. De Jaeghere W, De Beer T, Van Bocxlaer J, Remon JP, Vervaet C. Hot-melt extrusion of polyvinyl alcohol for oral immediate release applications. *Int J Pharm*. 2015; 492(1–2):1–9. [PubMed: 26160667]
13. Mohammed NN, Majumdar S, Singh A, Deng W, Murthy NS, Pinto E, et al. Klucel™ EF and ELF polymers for immediate-release oral dosage forms prepared by melt extrusion technology. *AAPS PharmSciTech*. 2012; 13(4):1158–69. [PubMed: 22961411]
14. Puri V, Brancazio D, Desai PM, Jensen KD, Chun JH, Myerson AS, et al. Development of maltodextrin-based immediate-release tablets using an integrated twin-screw hot-melt extrusion and injection-molding continuous manufacturing process. *J Pharm Sci*. 2017; 106(11):3328–36. [PubMed: 28684263]
15. Patil H, Tiwari RV, Upadhye SB, Vladyska RS, Repka MA. Formulation and development of pH-independent/dependent sustained release matrix tablets of ondansetron HCl by a continuous twin-screw melt granulation process. *Int J Pharm*. 2015; 496(1):33–41. [PubMed: 25863118]
16. Verstraete G, Van RJ, Van Bockstal PJ, et al. Hydrophilic thermoplastic polyurethanes for the manufacturing of highly dosed oral sustained release matrices via hot melt extrusion and injection molding. *Int J Pharm*. 2016; 506(1–2):214–21. [PubMed: 27113866]
17. Bhagurkar AM, Angamuthu M, Patil H, Tiwari RV, Maurya A, Hashemnejad SM, et al. Development of an ointment formulation using hot-melt extrusion technology. *AAPS Pharm Sci Tech*. 2016; 17(1):158–66.
18. Repka MA, McGinity JW. Influence of vitamin E TPGS on the properties of hydrophilic films produced by hot-melt extrusion. *Int J Pharm*. 2000; 202(1–2):63–70. [PubMed: 10915927]
19. Palem CR, Kumar Battu S, Maddineni S, Gannu R, Repka MA, Yamsani MR. Oral transmucosal delivery of domperidone from immediate release films produced via hot-melt extrusion technology. *Pharm Dev Technol*. 2013; 18(1):186–95. [PubMed: 22881235]

20. Mendonsa NS, Thipsay P, Kim DW, Martin ST, Repka MA. Bioadhesive drug delivery system for enhancing the permeability of a BCS class III drug via hot-melt extrusion technology. *AAPS PharmSciTech*. 2017; 18(7):2639–47. [PubMed: 28247291]
21. Patil H, Kulkarni V, Majumdar S, Repka MA. Continuous manufacturing of solid lipid nanoparticles by hot melt extrusion. *Int J Pharm*. 2014; 471(1–2):153–6. [PubMed: 24853459]
22. Ye X, Patil H, Feng X, Tiwari RV, Lu J, Gryczke A, et al. Conjugation of hot-melt extrusion with high-pressure homogenization: a novel method of continuously preparing nanocrystal solid dispersions. *AAPS Pharm Sci Tech*. 2016; 17(1):78–88.
23. Bruce LD, Shah NH, Malick AW, Infeld MH, McGinity JW. Properties of hot-melt extruded tablet formulations for the colonic delivery of 5-aminosalicylic acid. *Eur J Pharm Biopharm*. 2005; 59(1):85–97. [PubMed: 15567305]
24. Mehuys E, Remon JP, Vervaet C. Production of enteric capsules by means of hot-melt extrusion. *Eur J Pharm Sci*. 2005; 24(2–3):207–12. [PubMed: 15661492]
25. Castellsague J, Riera-Guardia N, Calingaert B, et al. Individual NSAIDs and upper gastrointestinal complications: a systematic review and meta-analysis of observational studies. *Drug Saf*. 2012; 35(12):1127–46. [PubMed: 23137151]
26. Henness S, Yang LP. Modified-release prednisone: in patients with rheumatoid arthritis. *Drugs*. 2013; 73(18):2067–76. [PubMed: 24249648]
27. Pozzi P, Furlani A, Gazzanig, Davis SS, Wilding IR. The time clock system: a new oral dosage form for fast and complete release of drug after a predetermined lag time. *J Control Release*. 1994; 31(1):99–108.
28. Yang R, Wang Y, Zheng X, Meng J, Tang X, Zhang X. Preparation and evaluation of ketoprofen hot-melt extruded enteric and sustained-release tablets. *Drug Dev Ind Pharm*. 2008; 34(1):83–9. [PubMed: 18214759]
29. Schilling SU, Shah NH, Waseem Malick A, McGinity JW. Properties of melt extruded enteric matrix pellets. *Eur J Pharm Biopharm*. 2010; 74(2):352–61. [PubMed: 19782133]
30. Andrews GP, Jones DS, Diak OA, McCoy CP, Watts AB, McGinity JW. The manufacture and characterisation of hot-melt extruded enteric tablets. *Eur J Pharm Biopharm*. 2008; 69(1):264–73. [PubMed: 18164604]
31. Dokoumetzidis A, Macheras P. A century of dissolution research: from Noyes and Whitney to the biopharmaceutics classification system. *Int J Pharm*. 2006; 321(1–2):1–11. [PubMed: 16920290]
32. Kalivoda A, Fischbach M, Kleinebudde P. Application of mixtures of polymeric carriers for dissolution enhancement of fenofibrate using hot-melt extrusion. *Int J Pharm*. 2012; 429(1–2):58–68. [PubMed: 22440149]
33. Zhang F. Melt-extruded Eudragit® FS-based granules for colonic drug delivery. *AAPS PharmSciTech*. 2016; 17(1):56–67. [PubMed: 26162974]

**Fig. 1.**

Schematic illustration of the screw configuration used for extrusion with a 16-mm extruder

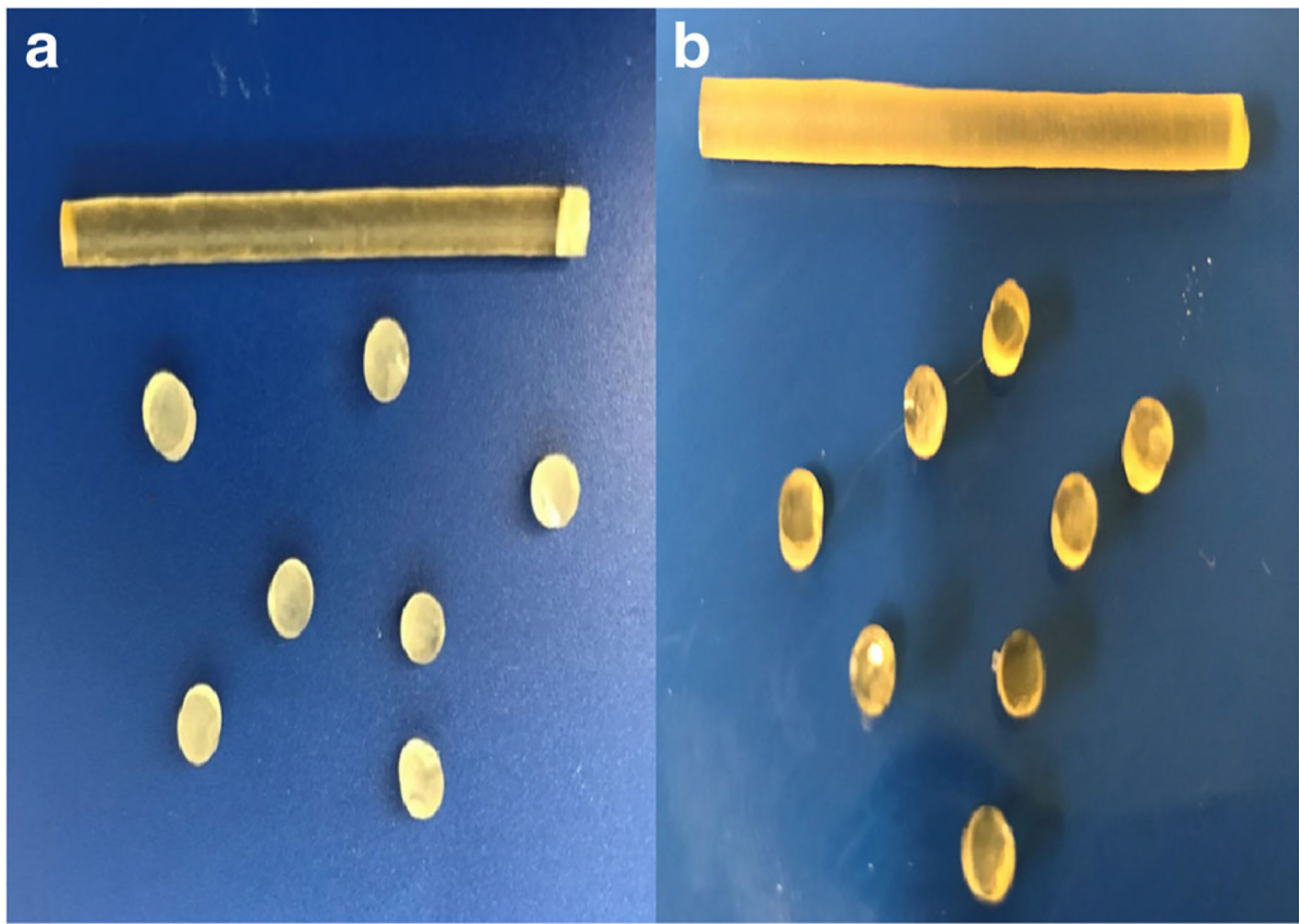


**Fig. 2.**

Images of extruded strands and pellets (3 mm) of KTP (a) and IBU (b)

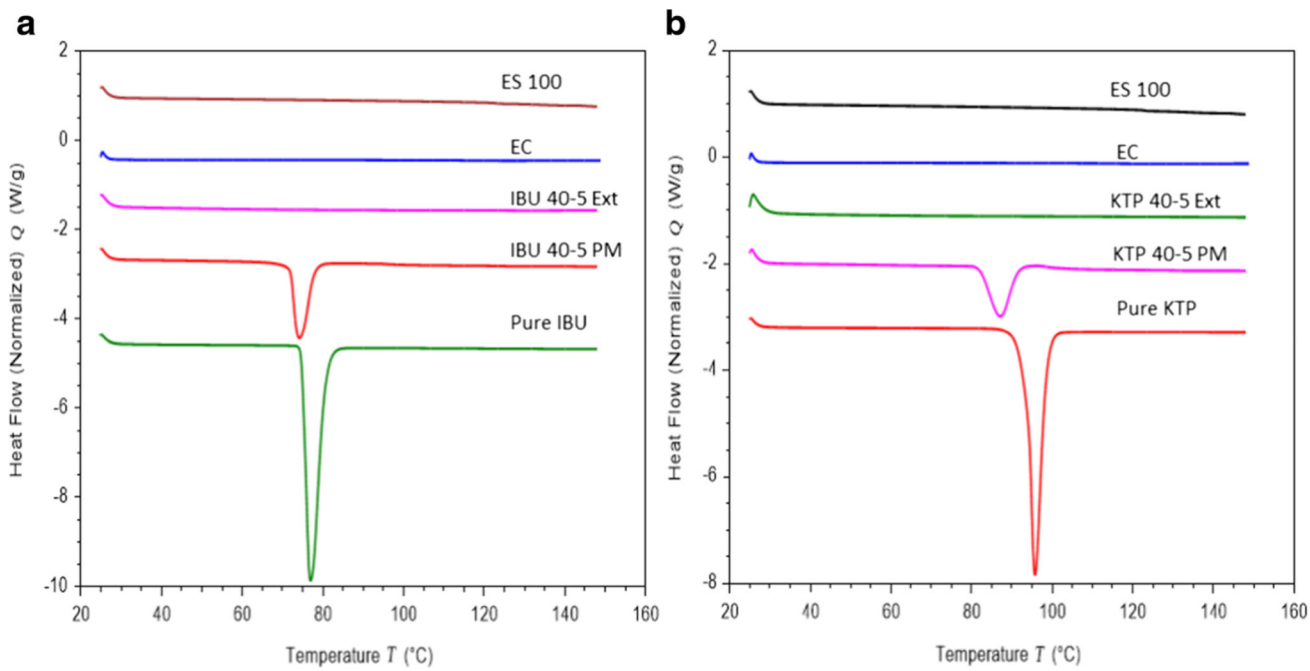


**Fig. 3.**  
DSC thermograms of (a) ES 100, EC, IBU 40-5Ext, IBU 40-5PM, Pure IBU (b) ES 100, EC, KTP 40-5Ext, KTP 40-5PM, Pure KTP

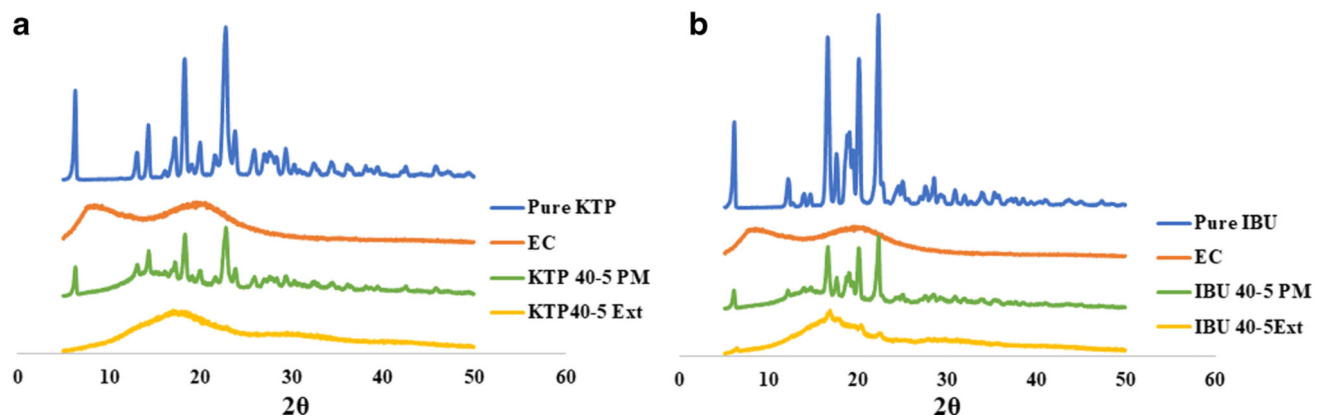


**Fig. 4.**  
PXRD of (a) EC, KTP 40-5 Ext, KTP 40-5PM, Pure KTP (b) EC, IBU 40-5Ext, IBU  
40-5PM, Pure IBU

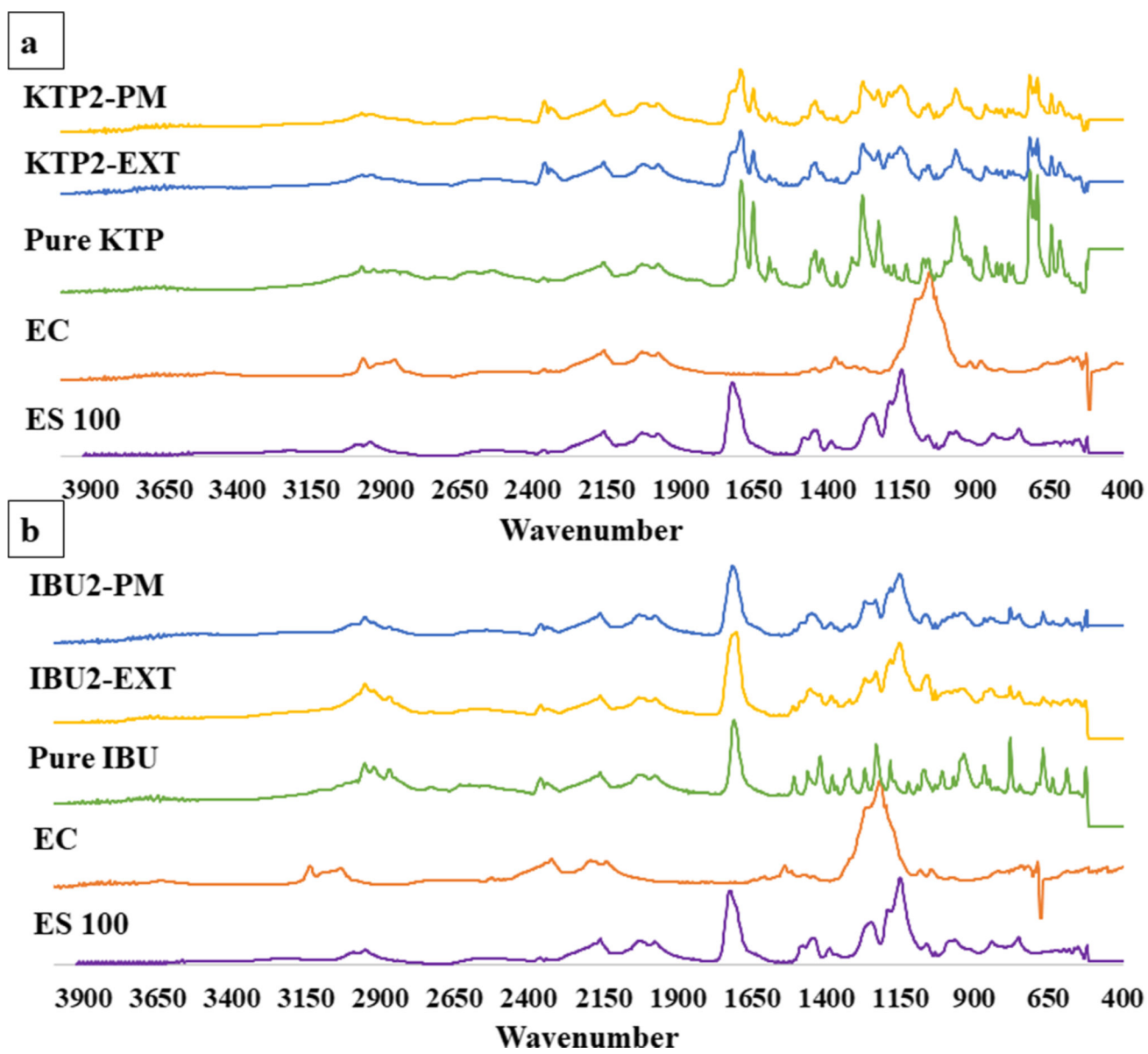


**Fig. 5.**  
FTIR spectra of KTP, IBU, polymers, physical mixtures (PM), and extrudate (EXT) formulations

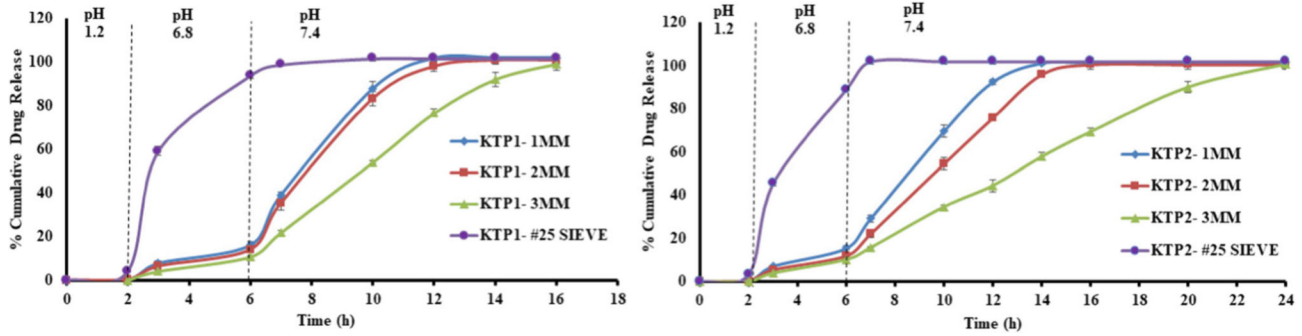


**Fig. 6.**

*In vitro* drug release profile of the KTP formulation containing 2.5% EC and 5% EC with different pellet sizes

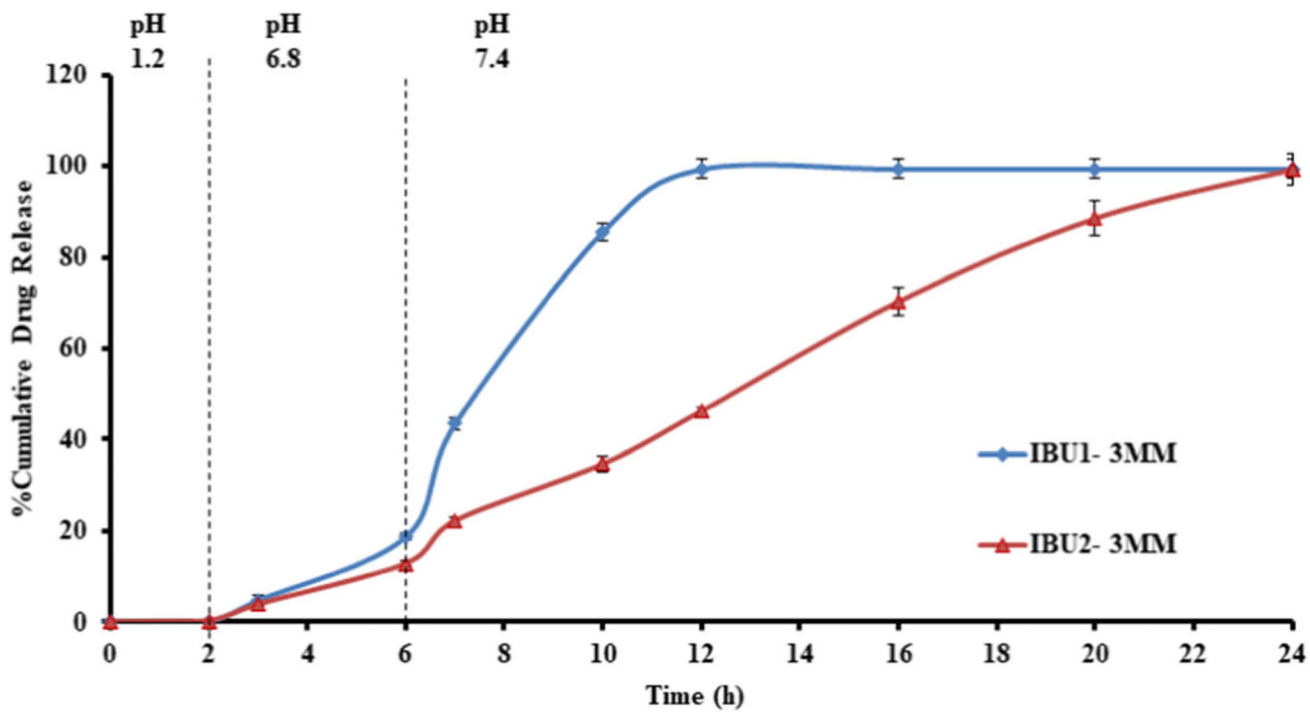


**Fig. 7.**

*In vitro* drug release profile of the IBU formulation containing 2.5% EC and 5% EC with 3 mm pellet size

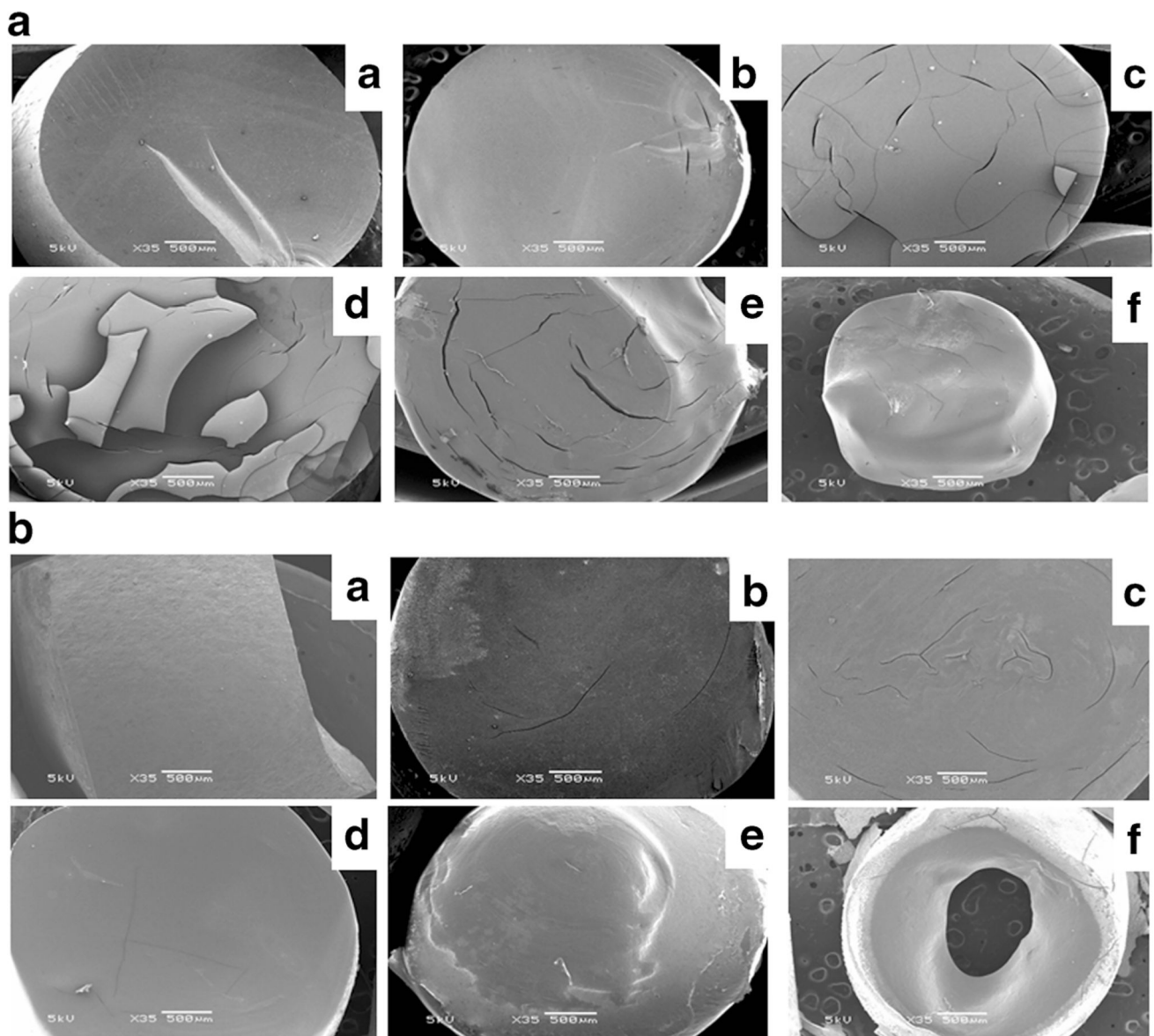


**Fig. 8.**

SEM images of (i) KTP and (ii) IBU pellets taken from dissolution media at different time points (a) 0 h, (b) 2 h, (c) 6 h, (d) 7 h, (e) 10 h, and (f) 12 h

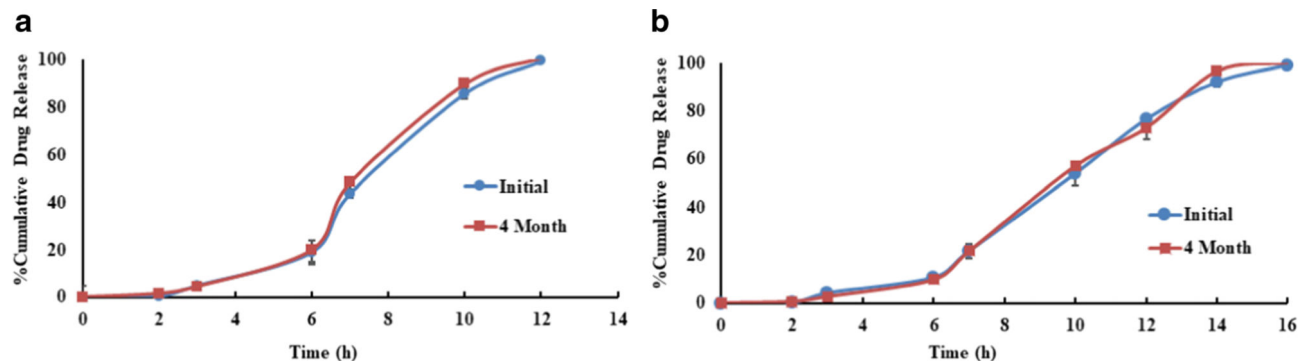


**Fig. 9.**

*In vitro* release profiles of IBU1-3MM (a) and KTP1-3MM (b) initially and after 4 months of accelerated stability study

**Table I**

Formulation Compositions, Processing Parameters, and Percent Drug Release at Lag Time of Initial Experiments with 6 mm Extruder

Formulation	KTP (%)	ES100 (%)	EC (%)	Temp (°C)	Torque (N cm)	% drug release at lag time (6 h)
1	30	70	0	130	110–120	50.3
2	40	60	0	120	80–85	55.8
3	50	50	0	120	60–70	NA <sup>a</sup>
4	20	70	10	145	100–110	4.4
5	20	75	5	145	100–110	5.9
6	20	77.5	2.5	145	100–110	6.4
7	30	65	5	130	110–120	11.8
8	30	67.5	2.5	130	110–120	17.2
9	40	55	5	120	80–90	13.0
10	40	57.5	2.5	120	85–90	18.8

<sup>a</sup>NA not applicable

Formulations and Processing Parameters of Final Formulations on 16 mm Extruder

Formulation	Drug (%)	ES100 (%)	EC (%)	Temp (°C)	Torque (%)
<b>Ketoprofen</b>					
KTP1	40	57.5	2.5	120	30
KTP2	40	55	5	120	35
<b>Ibuprofen</b>					
IBU1	40	57.5	2.5	100	40
IBU2	40	55	5	100	40